ECE 646 : Notes on the use of Angular Spectrum Model and Random Phase Screen

HTE – 31.03.2014

1. Angular Spectrum Model

For a given source beam of $u_s(s_x,s_y)$, we find the field on the receiver plane from the following Huygens-Fresnel integral

$$u_r(r_x,r_y,L)=\frac{-j}{\lambda L}\exp(j\frac{2\pi}{\lambda}L)\int_{-\infty}^{\infty}\int_{-\infty}^{\infty}ds_x ds_y u_s(s_x,s_y)\exp\left\{\frac{j\pi}{\lambda L}\left[(r_x-s_x)^2+(r_y-s_y)^2\right]\right\} \qquad (1.1)$$

where, s_x,s_y are the source plane coordinates, r_x,r_y are the receiver plane coordinates, λ is the emission wavelength of the optical source, L is the separation between source and receiver planes. Examining (1.1) more closely, we can see that it can be written as two dimensional convolution integral, that is

$$u_r(r_x,r_y,L)=u_s(s_x,s_y)\otimes h(r_x,\,r_y)=\int_{-\infty}^{\infty}\int_{-\infty}^{\infty}ds_x ds_y u_s(s_x,s_y)\;h(r_x-s_x,\,r_y-s_y) \qquad (1.2)$$

In (1.2), $\otimes$ is the convolution operator. By comparing (1.1) and (1.2), we get the spatial response of the propagating medium as

$$h(r_x,\,r_y)=\frac{-j}{\lambda L}\exp(j\frac{2\pi}{\lambda}L)\exp\left[\frac{j\pi}{\lambda L}\left(r_x^2+r_y^2\right)\right] \quad , \quad h(r_x-s_x,\,r_y-s_y)=\frac{-j}{\lambda L}\exp(j\frac{2\pi}{\lambda}L)\exp\left\{\frac{j\pi}{\lambda L}\left[(r_x-s_x)^2+(r_y-s_y)^2\right]\right\} \qquad (1.3)$$

In terms of Fourier transforms, (1.2) can also be written as

$$u_r(r_x,r_y,L)=\mathbf{F}^{-1}\left\{\mathbf{F}\left[u_s(s_x,s_y)\right]\mathbf{F}\left[h(r_x,\,r_y)\right]\right\}=\mathbf{F}^{-1}\left[U_s(f_x,f_y)H(f_x,f_y)\right] \qquad (1.4)$$

where $\mathbf{F}$ denotes the Fourier transform and $\mathbf{F}^{-1}$ denotes the inverse operator, f_x, f_y are the spatial frequencies. Finding the receiver plane field via the use of (1.4) is known as the angular spectrum method.

From (1.3), we find that

$$H(f_x, f_y) = \mathbf{F}\left[h(r_x,\, r_y)\right] = \exp(j\frac{2\pi}{\lambda}L)\exp\left[-j\pi\lambda L(f_x^2 + f_y^2)\right] \qquad (1.5)$$

(1.2) implies that (as an alternative to solving the Huygens Fresnel integral given in (1.1)), the field on the receiver plane can be evaluated by convolving the source plane field with the spatial response of the propagating medium, i.e., $h(r_x,\, r_y)$. Yet as a second alternative, using (1.4), we can obtain the receiver field expression, firstly by finding the Fourier transform of source field, then multiplying it by (1.5) and taking the inverse Fourier transform of the resulting expression. Although the Fourier transform method (angular spectrum model) seems to involve more steps and hence the expectation might be that this method would take longer time to execute, as will be seen later, the opposite is valid. This means the Fourier transform method is mostly preferred in practice than the convolutional method.

In (1.4), the use of arguments f_x, f_y both in $U_s(f_x, f_y)$ and $H(f_x, f_y)$ has the implication that the source and receiver coordinates are of the same scale or of the same increments. In practice, we know that this is not the case due to diffractive effects. To compensate for this, we introduce the following scaling factor

$$\mathbf{r} = \left(r_x, r_y\right) = m_f \mathbf{s} = m_f \left(s_x, s_y\right) \qquad (1.6)$$

Then following the derivation steps outlined in the notes entitled, “Notes on RPS derivations_27122012”, we have

$$u_r(r_x,r_y,L)=\exp(jkL)\exp\left[\frac{jk}{2L}\left(\frac{m_f-1}{m_f}\right)\left(r_x^2+r_y^2\right)\right]\mathbf{F}^{-1}\left\{\mathbf{F}\left[\frac{u_s\left(s_x,s_y\right)}{m_f}\exp\left[\frac{jk}{2L}\left(1-m_f\right)\left(s_x^2+s_y^2\right)\right]\right]\exp\left[-\frac{2j\pi^2L}{m_f k}\right]\left(f_x^2+f_y^2\right)\right\} \quad (1.7)$$

Example 1.1 : (1.7) is implemented in Matlab file, FTAngular.m where the intensity profile of one beam selected from range of hyperbolic and Gaussian beams are plotted using (1.7) and (5.18) of ECE 635_Free space propagation notes_Eylul 2011_HTE in the form of $I_r(r_x,r_y,L)=u_r(r_x,r_y,L)u_r^*(r_x,r_y,L)$, so that we can compare the results from the two cases. A sample reading for the cos Gaussian beam delivered from FTAngular.m is given in Fig. 1.1. In order to quantitatively assess the difference (as relative error, E) between the two results, we can compute

$$E=\left\{\sum_{r_x,r_y}^{N_g}\left[I_{ag}\left(r_x,r_y,L\right)-I_{an}\left(r_x,r_y,L\right)\right]^2\right\}^{0.5}/\left\{N_g^2 Max\left[I_{ag}\left(r_x,r_y,L\right),I_{an}\left(r_x,r_y,L\right)\right]\right\} \quad (1.7)$$

where $I_{ag}\left(r_x,r_y,L\right)$ is the intensity found by using the angular spectrum method described above, $I_{an}\left(r_x,r_y,L\right)$ is the intensity found by the analytic formulation given in (5.18) of ECE 635_Free space propagation notes_Eylul 2011_HTE, N_g represents the number of grid points on the receiver transverse planes, in this example it is set to 512.

Exercise 1.1 : By using FTAngular.m, test for other beams to see how much difference or error there is between $I_{ag}\left(r_x,r_y,L\right)$ and $I_{an}\left(r_x,r_y,L\right)$. Do this at least at ten other source and propagation settings, such as change of beam type, source size, displacement parameter, propagation

length. Note that depending on the these settings, source and receiver planes side lengths may have to be adjusted, these settings are on line 8 of the code FTAngular.m.

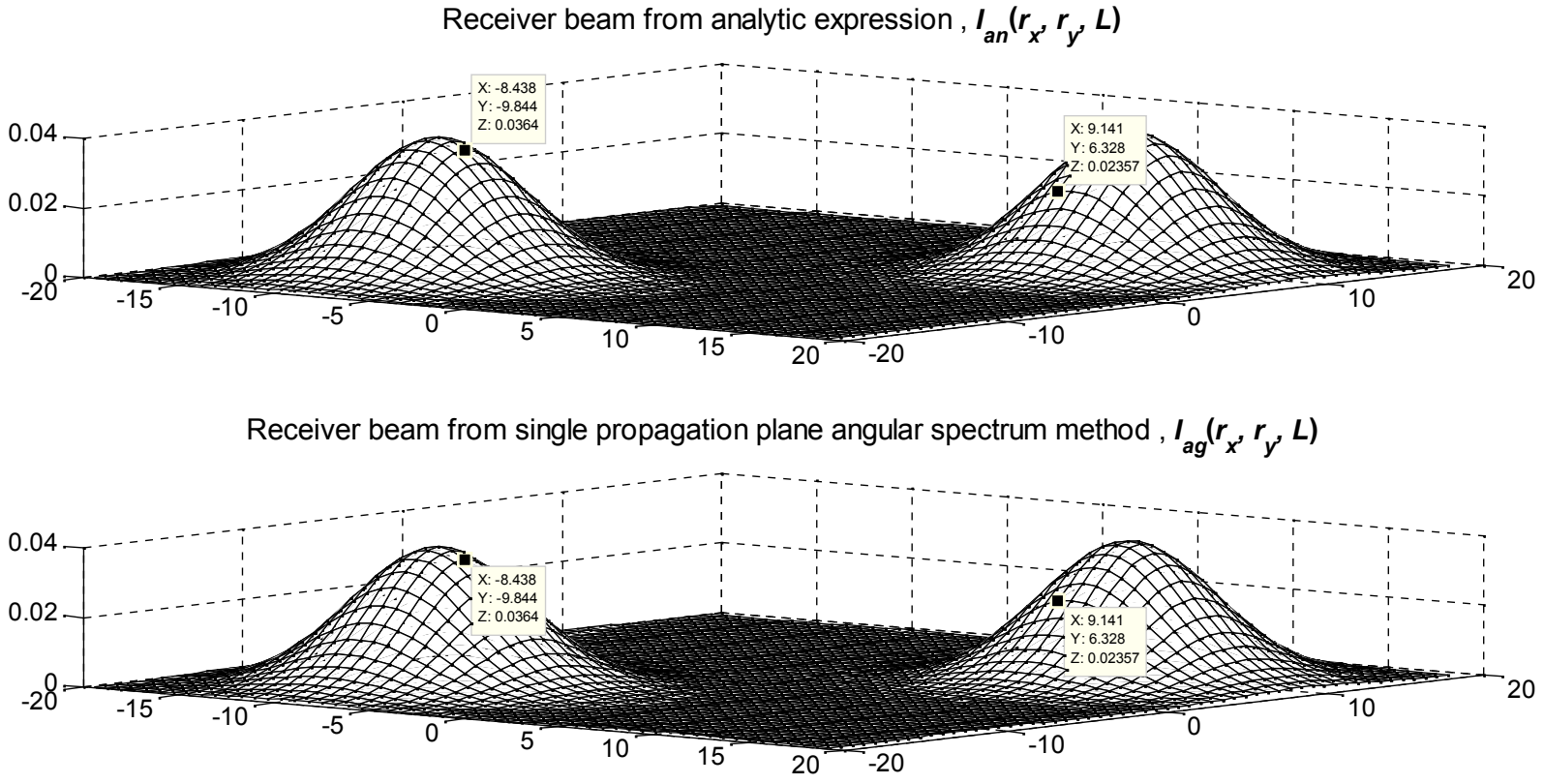

Fig. 1.1 Comparison of beam profiles of cos Gaussian beam from analytic formulation and the angular spectrum method. The source and propagation settings are $\alpha_{sx} = \alpha_{sy} = 1$ cm, $D_x = D_y = 2$ cm^{-1}, $\lambda = 1.55$ μm, $L = 2$ km, $L_s = 10$ cm, $L_r = 40$ cm .

Now we turn to the convolution application of (1.2), which is handled in ConvNS.m. An output of the same beam as in Fig. 1.1 is given in Fig. 1.2.

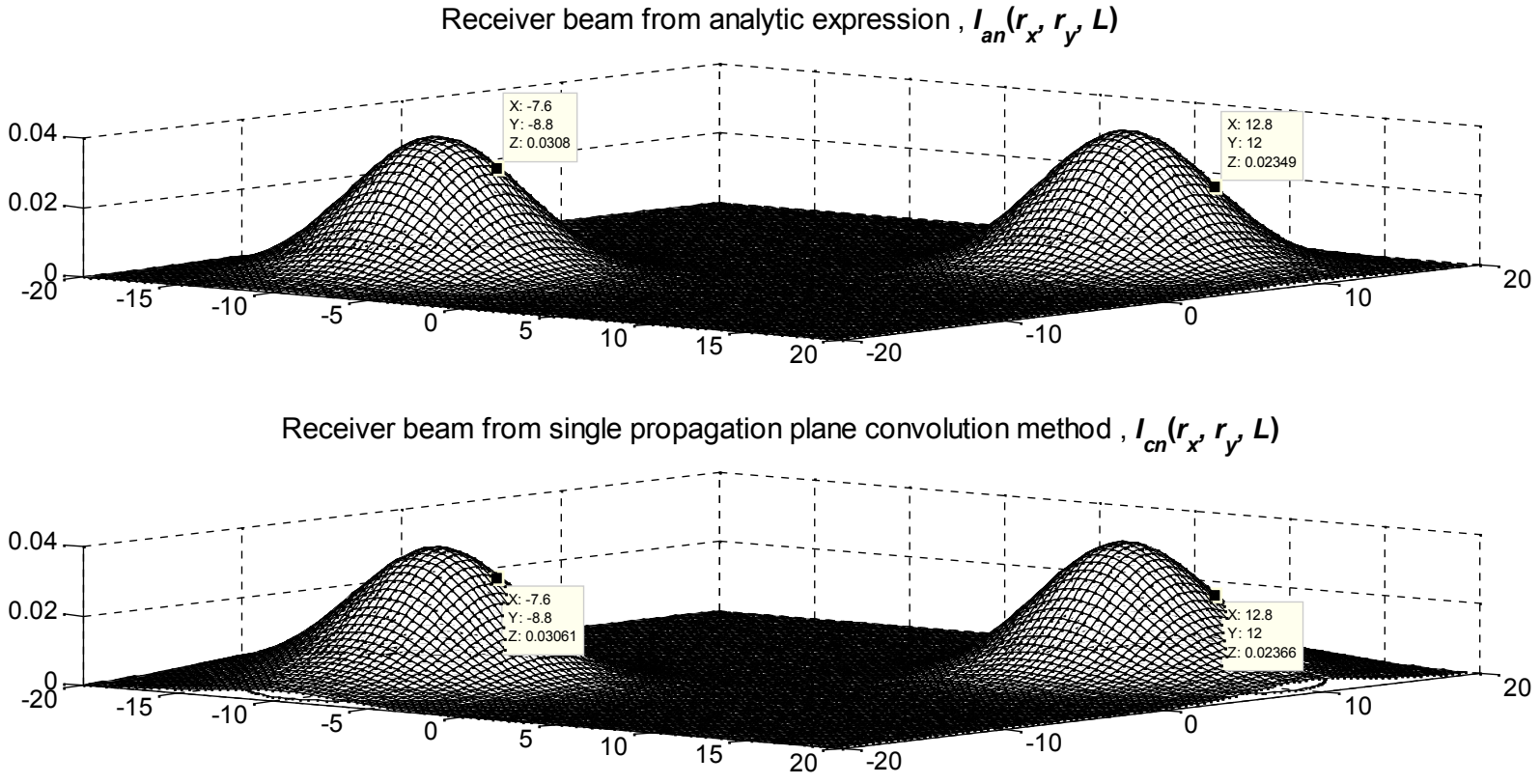

Fig. 1.2 Comparison of beam profiles of cos Gaussian beam from analytic formulation and the convolution method. The source and propagation settings are $\alpha_{sx} = \alpha_{sy} = 1$ cm, $D_x = D_y = 2$ cm^{-1}, $\lambda = 1.55$ μm, $L = 2$ km, $L_s = 10$ cm, $L_r = 40$ cm .

The data cursor values in Fig. 1.2 for analytic and convolution methods are no longer in perfect agreement. This can be better judged by comparing the respective errors as defined in (1.7). As written out onto the workspace, these are

$$E\left(\text{for angular spectrum method}\right)=3.1994\times10^{-5}\ ,\ E\left(\text{for convolution method}\right)=0.0013 \qquad (1.8)$$

Of course, the number of grid points, N_g is highly different in the two case, i.e.,

$$N_g\left(\text{for angular spectrum method}\right)=512\ ,\ N_g\left(\text{for convolution method}\right)=100 \qquad (1.9)$$

It should be pointed out that, if $N_g\left(\text{for convolution method}\right)=512$ is used, the computation time for convolution method becomes excessive. In the angular spectrum method, since Matlab embedded FFT is used, the computation time is quite reasonable.

Exercise 1.2 : By using ConvNS.m, test for other beams to see how much difference or error there is between $I_{cn}\left(r_x,r_y,L\right)$ and $I_{an}\left(r_x,r_y,L\right)$, where $I_{ag}\left(r_x,r_y,L\right)$ is the intensity found by convolution method. Do this at least at ten other source and propagation settings, such as change of beam type, source size, displacement parameter, propagation length. Note that depending on the these settings, source and receiver planes side lengths may have to be adjusted, these settings are on line 7 of the code ConvNS.m.

2. Random Phase Screen Model

The angular spectrum method described above can be integrated into another representation to model the propagation in turbulence. For this two new steps have to be introduced

a) A total of some random phase screens, say N_s, must be placed between the source and receiver planes in order to model the atmospheric turbulence. The random phase distributions on these screens are to be in proportion to atmospheric power spectral density function.

b) A number of realizations (runs), say N_R must be made to approach the averaged analytic result.

The requirement a) can be fulfilled by placing a number of phase screens between the source and the receiver planes as shown in Fig. 2.1.

As seen from Fig. 2.1, the propagation can be handled partly by angular spectrum method (in between the phase screens) and then the accumulated effect of turbulence can be incorporated by the next random phase screen. This way assuming that there are N_s number of phase screens from the source plane to the receiver plane, then in going from $(n-1)$ th screen to the n th one, (1.4) of above will turn into

$$u_r(r_x,r_y,n\Delta L)=\mathbf{F}^{-1}\left(\mathbf{F}\left\{u_r\left[r_x,r_y,(n-1)\Delta L\right]\exp\left[j\phi\left(r_x,r_y\right)\right]\right\}H\left(f_x,f_y\right)\right) \qquad (2.1)$$

where $\phi\left(r_x,r_y\right)$ denotes the spatial phase distribution derived from the power spectral density function. Fig. 2.1 and (2.1) imply that in contrast to the utilization of angular spectrum model in free space propagation, the propagation in turbulence via random phase screens will involve split step or multi hop propagation arrangement. In this process, the scaling factor, m_f between the source and the receiver planes must be adjusted accordingly.

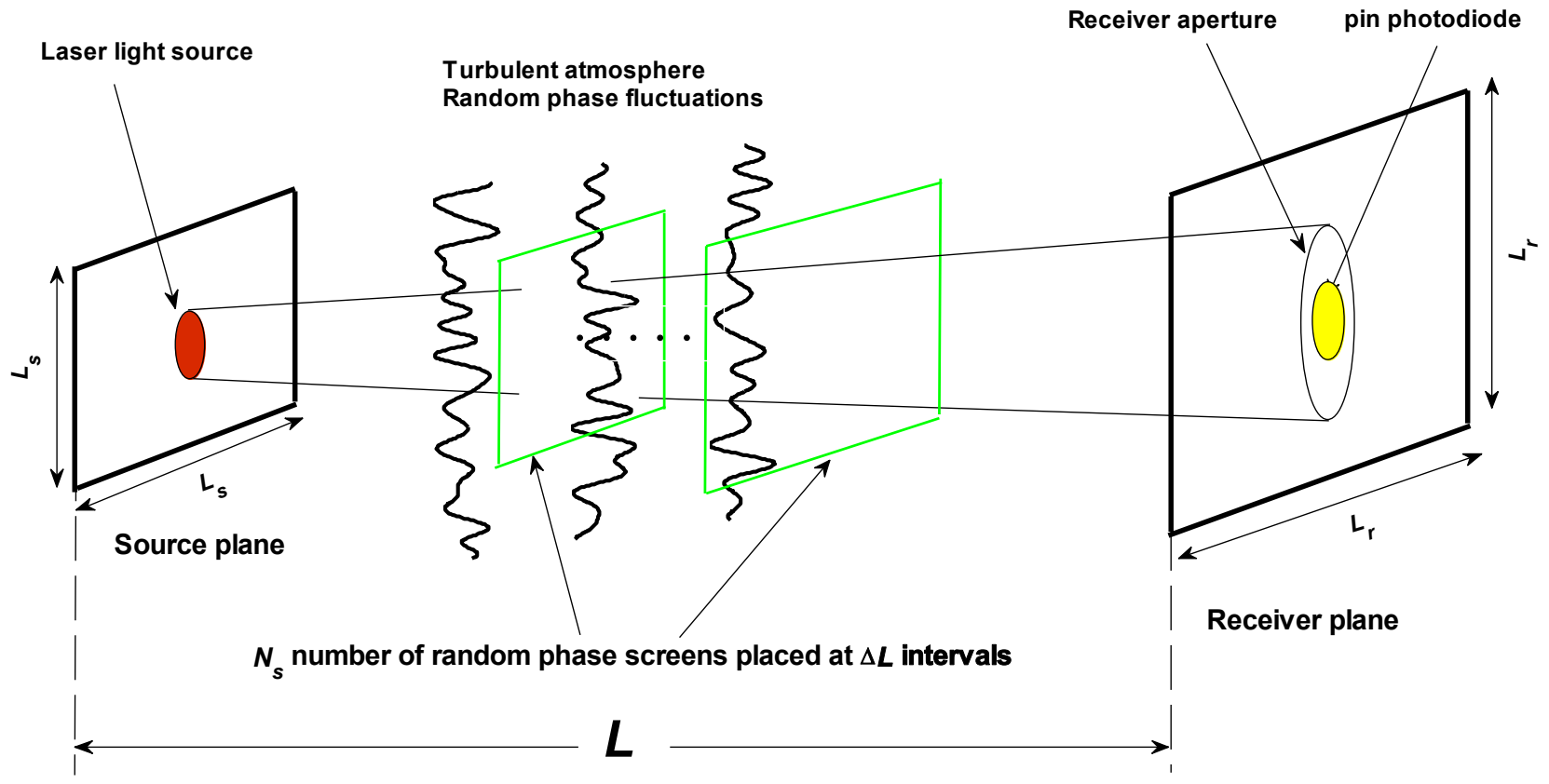

Fig. 2.1 Pictorial view of modelling propagation in turbulence via random phase screens.

In Fig. 2.2, we illustrate the 3D intensity profiles obtained by running the Matlab file, RPS_Int_APAV.m in Fig. 2.2 and its cross sectional 2D view in Fig. 2.3.

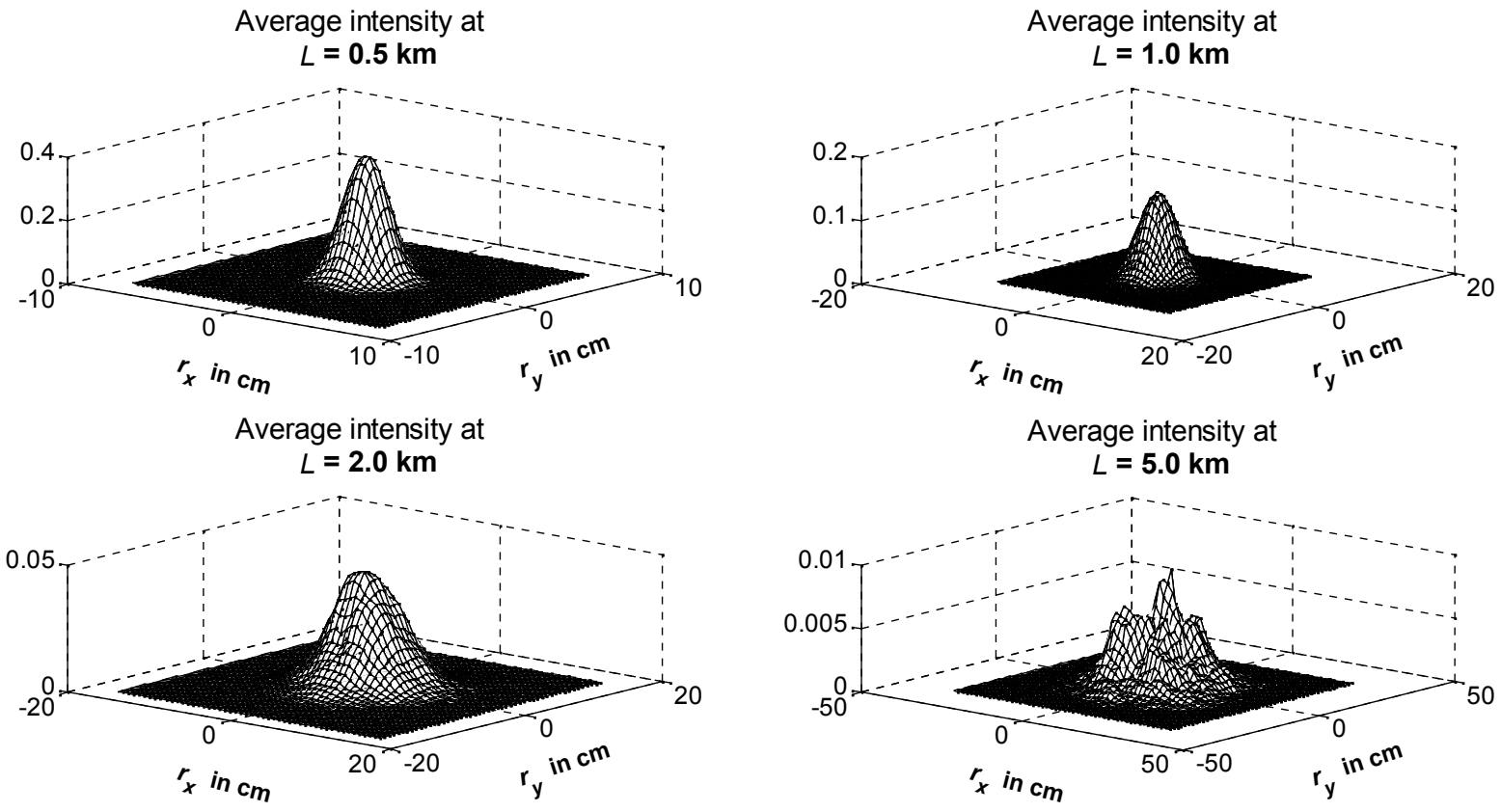

Fig. 2.2 Gaussian beam 3D intensity profiles at several propagation distances. The source and propagation settings are

$\alpha_{sx} = \alpha_{sy} = 1$ cm, $\lambda = 1.55$ μm, $N_s = 21$, $N_R = 2$, $C_n^2 = 10^{-15}$ m$^{-2/3}$, $L_s = 10$ cm .

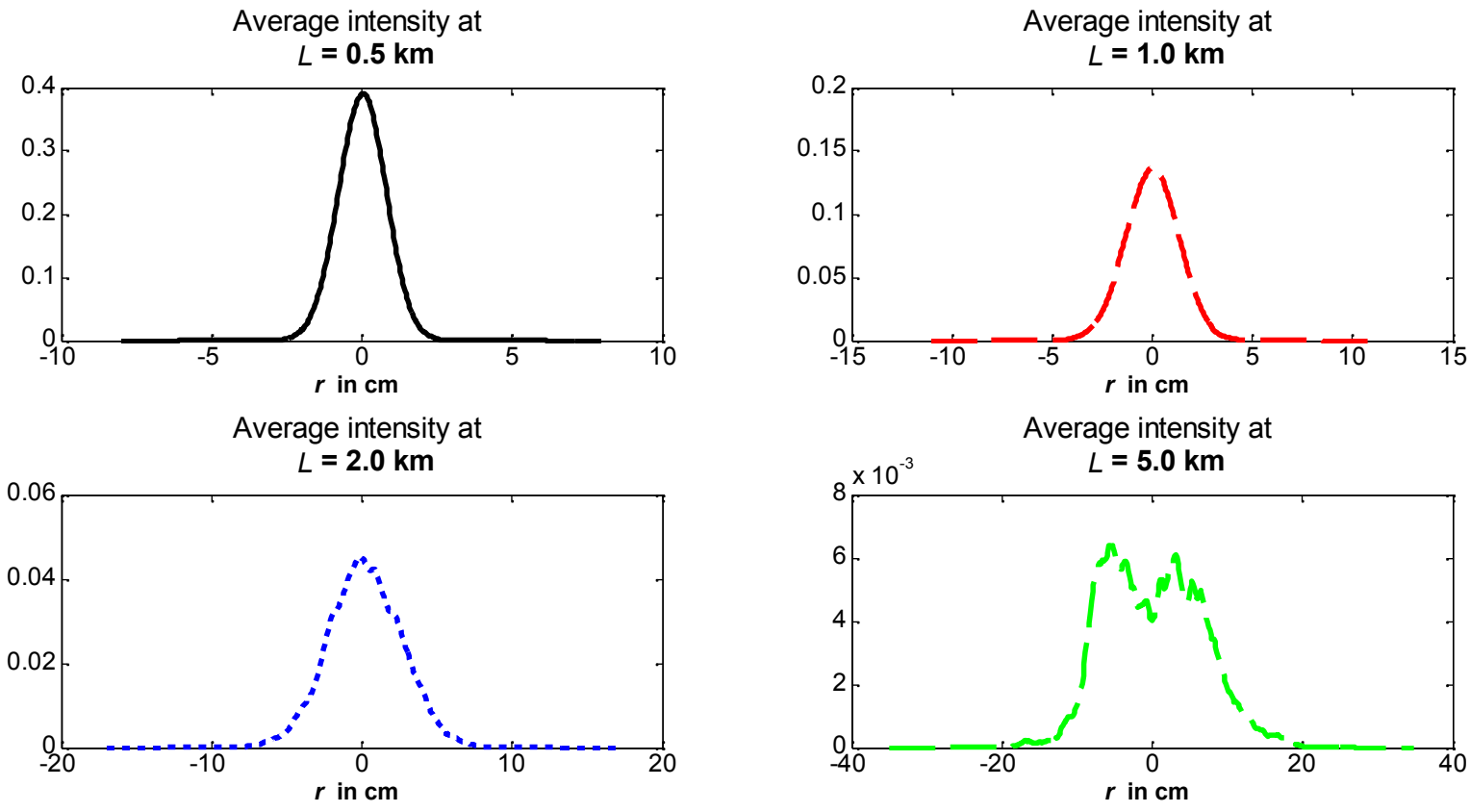

Fig. 2.3 Gaussian beam 2 D intensity profiles at several propagation distances. The source and propagation settings are

$\alpha_{sx} = \alpha_{sy} = 1$ cm, $\lambda = 1.55$ μm, $N_s = 21$, $N_R = 2$, $C_n^2 = 10^{-15}$ m$^{-2/3}$, $L_s = 10$ cm .

Exercise 2.1 : Using the same Matlab file, i.e., RPS_Int_APAV.m, obtain results similar to Figs. 2.2 and 2.3. In particular investigate the dependence of intensity profiles on $N_R = 2$ and beam types.

3. Pointlike and Aperture Averaged Scintillation

One attractive feature of obtaining the receiver plane fields and consequently the intensities is that evaluation of scintillation index, which here we call pointlike scintillation and aperture averaged scintillation, otherwise known as power scintillation. From (3.23) of Notes of ECE 646_HTE_Bahar 2012, we know that scintillation index is given by

$$m^2\left(r_x, r_y, L\right) = \frac{\left\langle I^2\left(r_x, r_y, L\right)\right\rangle}{\left\langle I\left(r_x, r_y, L\right)\right\rangle^2} - 1 \qquad (3.1)$$

(3.1) defines the scintillation index at a specific location on the receiver plane, i.e. at $\left(r_x, r_y\right)$. As shown in Fig. 2.1, the optical receivers usually have a finite circular aperture opening. Assuming the radius of this aperture is R_a, then according to the literature, (3.1) will be valid so long as $R_a < \sqrt{0.5\lambda L/\pi}$, otherwise apertured averaged scintillation or power scintillation will occur, defined as

$$b^2(L) = \frac{\left\langle P^2(L)\right\rangle}{\left\langle P(L)\right\rangle^2} - 1 \quad , \quad P(L) = \int_{-0.5\sqrt{\pi}R_a}^{0.5\sqrt{\pi}R_a} \int_{-0.5\sqrt{\pi}R_a}^{0.5\sqrt{\pi}R_a} I\left(r_x, r_y, L\right) dr_x dr_y \qquad (3.2)$$

where $P(L)$ refers to power of the beam at a propagation distance of L captured by a circular aperture of radius R_a and $0.5\sqrt{\pi}R_a$ is the Cartesian equivalent of side length of the square shaped aperture.

It is quite easy to evaluate (3.1) and (3.2) when propagation in turbulence is modelled by random phase screens. For (3.1), we do this by choosing a small aperture, where $R_a < \sqrt{0.5\lambda L/\pi}$ is well satisfied and finding the power over this small aperture by applying the double integration in

(3.2), thus acquiring $P(L)$. From there it is easy to find $\langle P^2(L)\rangle$ and $\langle P(L)\rangle^2$, consequently $b^2(L)$ by running N_R number of realizations. Note that here we have actually reached apertured averaged power scintillation parameter, $b^2(L)$. But under the conditions of $R_a < \sqrt{0.5\lambda L/\pi}$, we have assumed that $m^2(r_x, r_y, L) \simeq b^2(L)$. It is important to point out that the aperture averaging phenomenon is an important act that it brings substantial scintillation reductions as will be demonstrated below.

In Fig. 3.1, the pointlike scintillation index of a Gaussian beam is displayed, by running the Matlab file RPS_Int_APAV.m, that contains the random phase screen setup of Fig. 2.1. The circular equivalent aperture radius here is, $R_a = 0.22$ cm. On the other hand, at $L = 5$ km, $\sqrt{0.5\lambda L/\pi} = 3.51$ cm, therefore the condition $R_a < \sqrt{0.5\lambda L/\pi}$ is well satisfied. I n this manner, the scintillation index values on the curve of Fig. 3.1 are well in agreement with the Gaussian curve of Fig. 1 of the article, "A16_Scintillation characteristics of cosh-Gaussian beams_AO_2007_Pub Ver".

Next in Fig. 3.2, we set circular equivalent aperture radius to $R_a = 3.08$ cm. Since here $R_a \approx \sqrt{0.5\lambda L/\pi}$, we obtain nearly apertured average scintillation, thus in comparison to Fig. 3.1, scintillation reductions are observed in Fig. 3.2. Eventually in Fig. 3.3, we have increased circular equivalent aperture radius to $R_a = 6.24$ cm, where $R_a > \sqrt{0.5\lambda L/\pi}$ is well satisfied. In the manner, Fig. 3.3 illustrates in a clear manner the advantages of apertured averaged scintillation, both in comparison to Figs. 3.1 and 3.2.

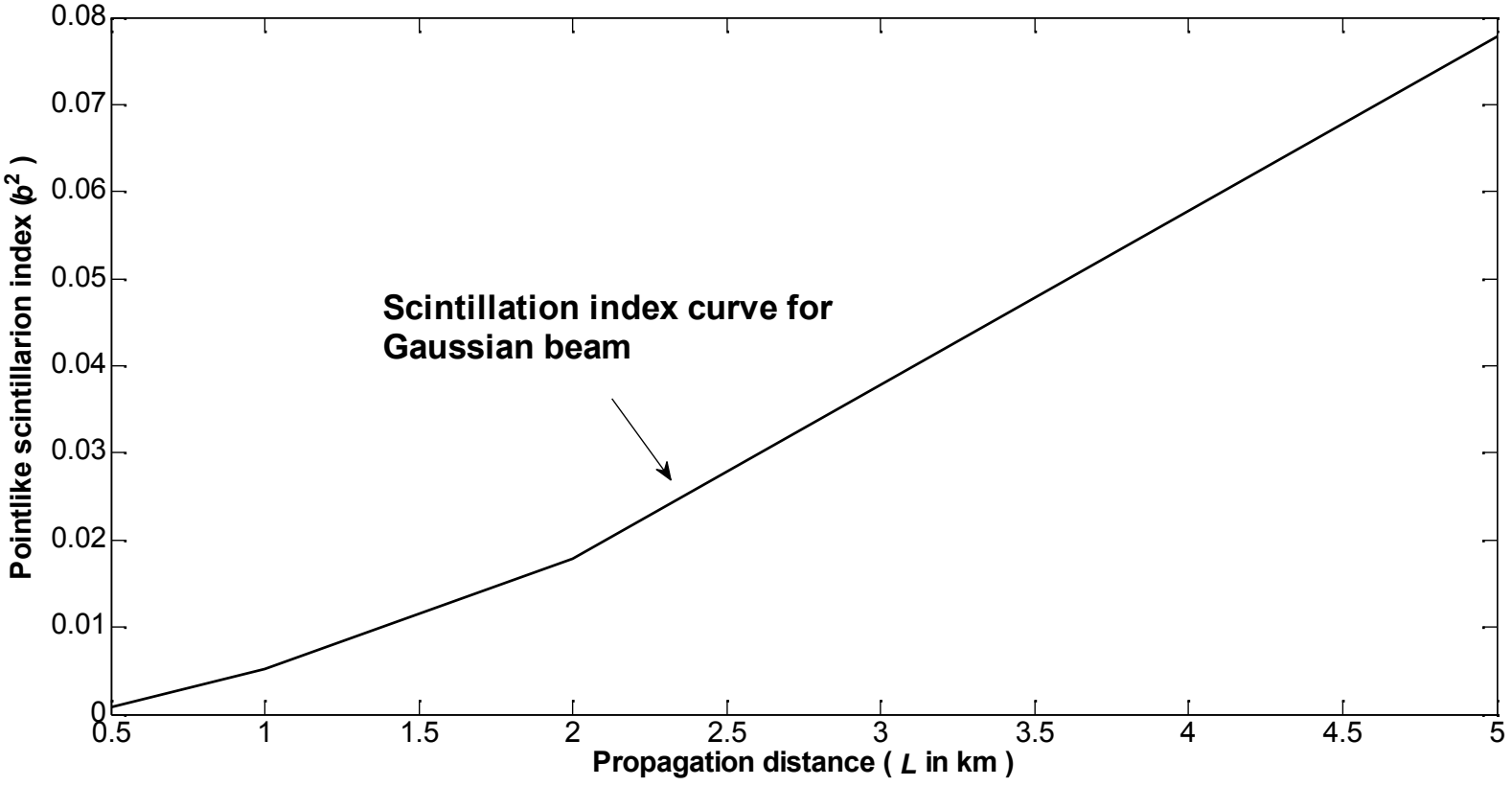

Fig. 3.1 Pointlike scintillation index of Gaussian beams. The source and propagation settings are

$\alpha_{sx} = \alpha_{sy} = 1$ cm, $\lambda = 1.55$ μm, $N_s = 21$, $N_R = 10$, $C_n^2 = 10^{-15}$ m$^{-2/3}$, $L_s = 10$ cm, $L_r = 71.68$ cm, at $L = 5$ km, $R_a = 0.22$ cm, $\sqrt{0.5\lambda L/\pi} = 3.51$ cm.

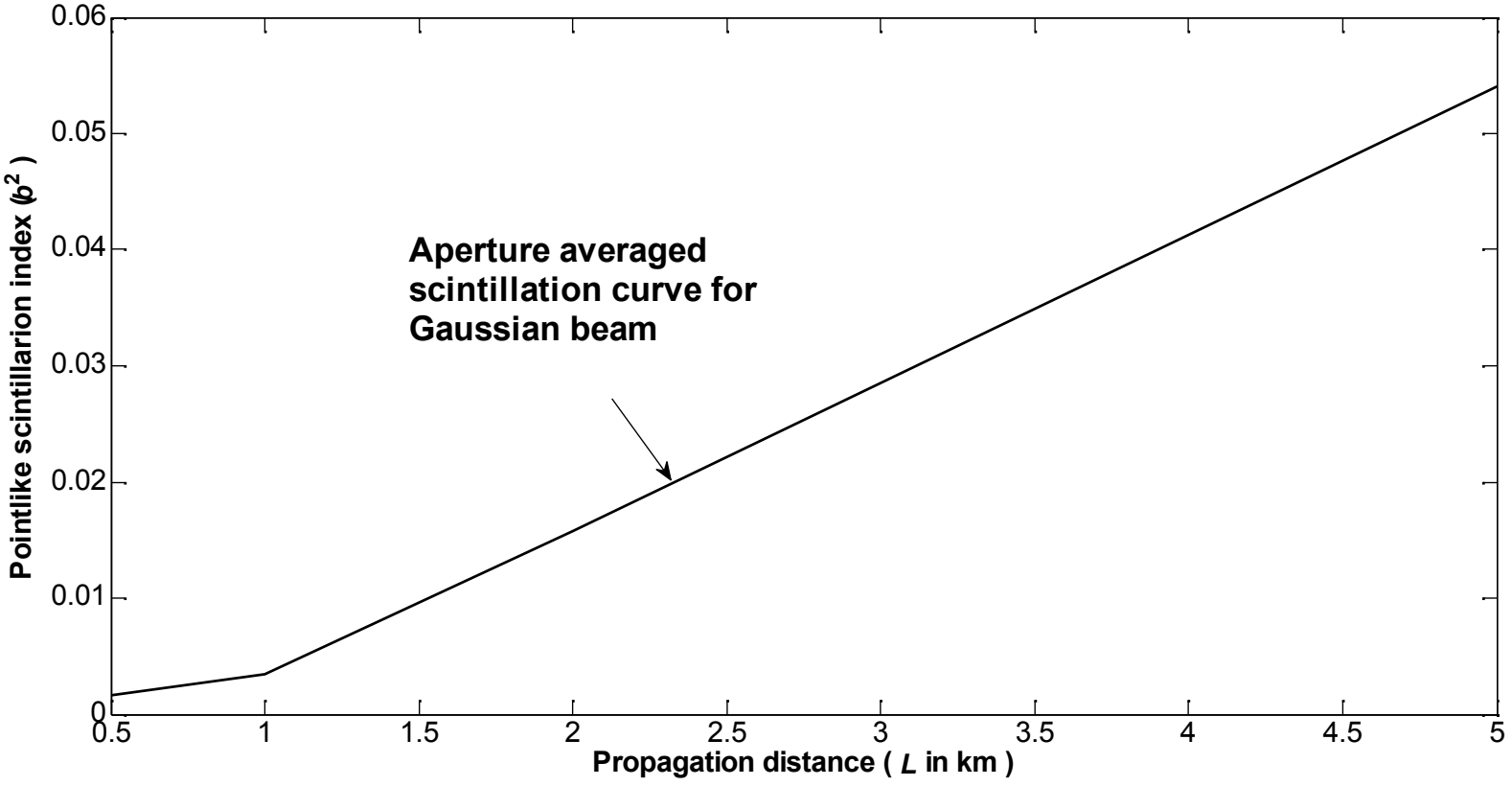

Fig. 3.2 Aperture averaged scintillation of Gaussian beams. The source and propagation settings are

$\alpha_{sx} = \alpha_{sy} = 1$ cm, $\lambda = 1.55$ μm, $N_s = 21$, $N_R = 10$, $C_n^2 = 10^{-15}$ m$^{-2/3}$, $L_s = 10$ cm, $L_r = 71.68$ cm, at $L = 5$ km, $R_a = 3.02$ cm, $\sqrt{0.5\lambda L/\pi} = 3.51$ cm.

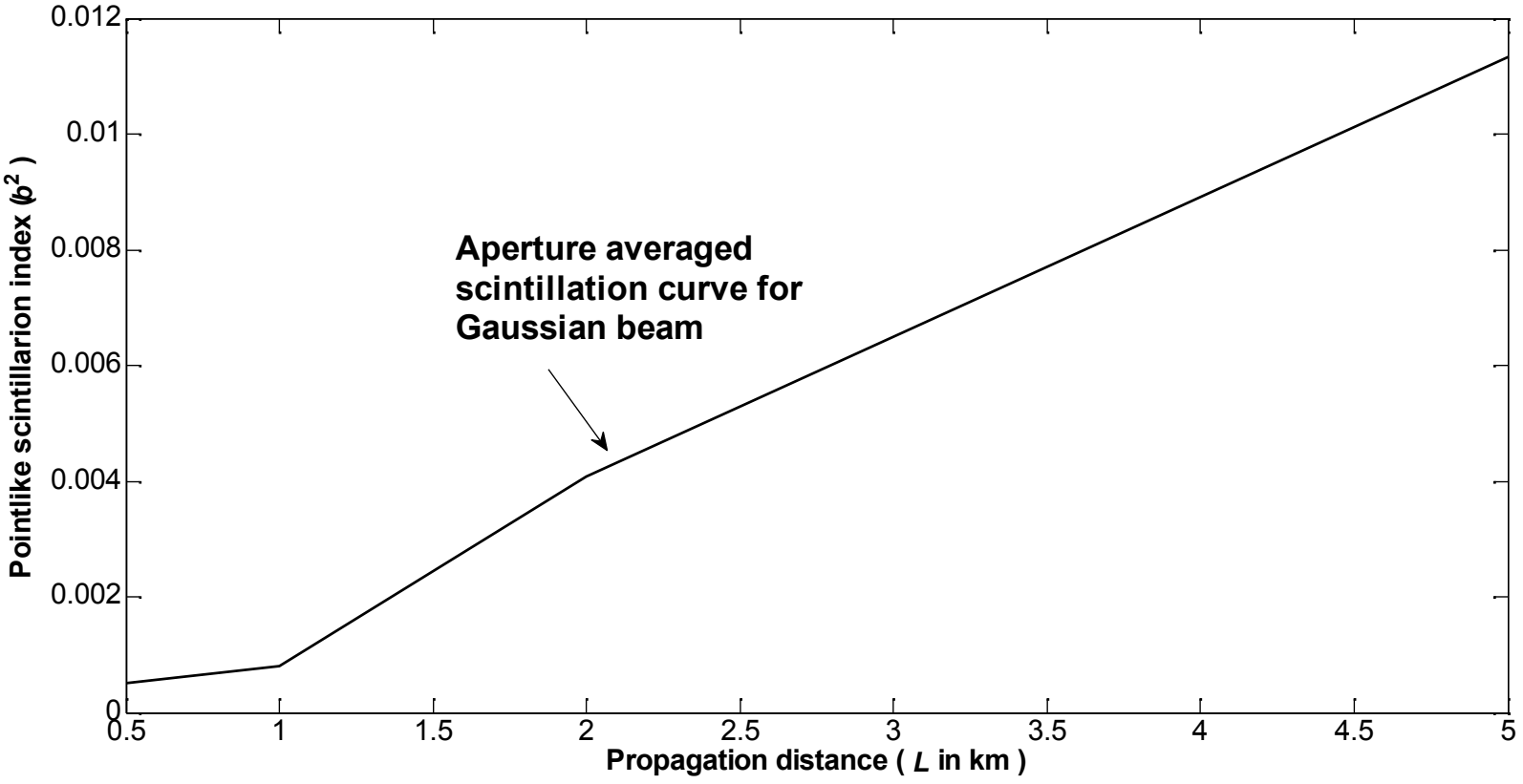

Fig. 3.2 Aperture averaged scintillation of Gaussian beams. The source and propagation settings are

$\alpha_{sx} = \alpha_{sy} = 1$ cm, $\lambda = 1.55$ μm, $N_s = 21$, $N_R = 10$, $C_n^2 = 10^{-15}$ m$^{-2/3}$, $L_s = 10$ cm, $L_r = 71.68$ cm, at $L = 5$ km, $R_a = 6.24$ cm, $\sqrt{0.5\lambda L/\pi} = 3.51$ cm.

Exercise 3.1 : By using Matlab file RPS_Int_APAV.m (together with ft_sh_phase_screen.m) to obtain scintillation plots of other sinusoidal hyperbolic Gaussian beams and compare your pointlike scitillation results with the graphs given in the articles, "A15_Scintillation of cos and annular beams_JOSA A 2007_Pub ver" and "A16_Scintillation characteristics of cosh-Gaussian beams_AO_2007_Pub Ver".